



Deposited via The University of Sheffield.

White Rose Research Online URL for this paper:

<https://eprints.whiterose.ac.uk/id/eprint/158040/>

Version: Published Version

---

**Article:**

Jiang, S., Cai, Y., Feng, P. et al. (2020) Exploring an approach toward the intrinsic limits of GaN electronics. *ACS Applied Materials & Interfaces*, 12 (11). pp. 12949-12954. ISSN: 1944-8244

<https://doi.org/10.1021/acsami.9b19697>

---

**Reuse**

This article is distributed under the terms of the Creative Commons Attribution (CC BY) licence. This licence allows you to distribute, remix, tweak, and build upon the work, even commercially, as long as you credit the authors for the original work. More information and the full terms of the licence here:

<https://creativecommons.org/licenses/>

**Takedown**

If you consider content in White Rose Research Online to be in breach of UK law, please notify us by emailing [eprints@whiterose.ac.uk](mailto:eprints@whiterose.ac.uk) including the URL of the record and the reason for the withdrawal request.

# Exploring an Approach toward the Intrinsic Limits of GaN Electronics

Sheng Jiang,<sup>‡</sup> Yuefei Cai,<sup>‡</sup> Peng Feng, Shuoheng Shen, Xuanming Zhao, Peter Fletcher, Volkan Esendag, Kean-Boon Lee, and Tao Wang\*

Cite This: *ACS Appl. Mater. Interfaces* 2020, 12, 12949–12954

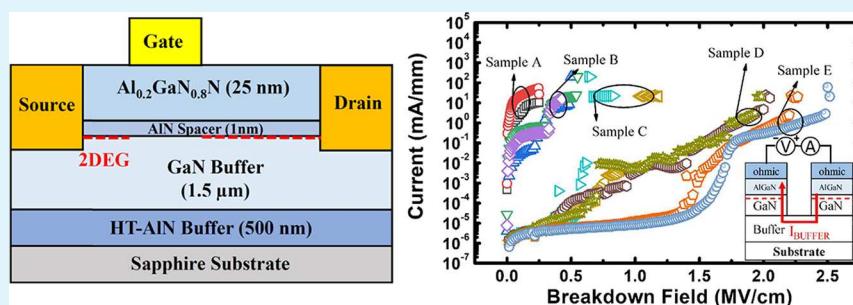
Read Online

ACCESS |

Metrics & More

Article Recommendations

Supporting Information



**ABSTRACT:** To fully exploit the advantages of GaN for electronic devices, a critical electric field that approaches its theoretical value (3 MV/cm) is desirable but has not yet been achieved. It is necessary to explore a new approach toward the intrinsic limits of GaN electronics from the perspective of epitaxial growth. By using a novel two-dimensional growth mode benefiting from our high-temperature AlN buffer technology, which is different from the classic two-step growth approach, our high-electron-mobility transistors (HEMTs) demonstrate an extremely high breakdown field of 2.5 MV/cm approaching the theoretical limit of GaN and an extremely low off-state buffer leakage of 1 nA/mm at a bias of up to 1000 V. Furthermore, our HEMTs also exhibit an excellent figure-of-merit ( $V_{br}^2/R_{on,sp}$ ) of  $5.13 \times 10^8 \text{ V}^2/\Omega\text{-cm}^2$ .

**KEYWORDS:** GaN, breakdown voltage, critical electric field, HEMTs, leakage current, 2DEG, electronics, MOVPE growth

## INTRODUCTION

Intrinsic GaN with inherent polarization on *c*-plane substrates is supposed to exhibit superior electrical properties to almost all of the other existing semiconductors, such as high electron mobility and a very high sheet carrier density of two-dimensional electron gas (2DEG) formed in an AlGaIn/GaN heterostructure but without using any modulation doping<sup>1,2</sup> and high breakdown voltage (with the theoretical value of the critical electrical field of  $\sim 3\text{MV/cm}$ ).<sup>3,4</sup> Due to its wide band gap, intrinsic GaN is supposed to be at least semi-insulating. Despite significant progress obtained in the last two decades, the performance of GaN electronic devices is far from the limits of this material, which we believe is due to the challenges in material growth. Therefore, it is crucial to understand the fundamental issues from the perspective of epitaxial growth and then to explore a new approach toward these theoretical limits.

Currently, a standard growth approach for GaN grown on sapphire is based on the classic two-step method developed by three 2014 Nobel Prize Laureates Akasaki, Amano, and Nakamura by using metal–organic vapor-phase epitaxy (MOVPE) techniques; namely, a thin GaN or AlN nucleation layer is initially prepared at a low temperature (LT) followed

by a thick GaN buffer layer grown at a high temperature prior to the growth of any further device structures. In terms of growth modes, this approach is based on the initial formation of small islands on a nanometer scale evolved from the LT nucleation layer due to a subsequent annealing process followed by a gradual coalescence process to finally obtain a flat surface (i.e., initially a three dimensional (3D) growth mode and then a 2D growth mode). This two-step growth approach has resulted in major improvement in the crystal quality of GaN in the last two decades, leading to unprecedented success in the field of III-nitride optoelectronics. However, this growth approach poses a great challenge in obtaining a semi-insulating GaN buffer layer, which is crucial for the growth of GaN electronics.<sup>5–7</sup> The GaN buffer grown by using the two-step method exhibits severe current leakage as a result of its low resistivity. In order to address this issue, a

Received: October 31, 2019

Accepted: February 24, 2020

Published: February 24, 2020

carbon-doped (C-doped) GaN buffer approach still based on the two-step method has been widely adopted for the growth of AlGaIn/GaN-based high-electron-mobility transistors (HEMTs) as C-doped GaN, which can be obtained by growing nominally undoped GaN at a low temperature, has been proven to be efficient to suppress a buffer leakage based on a compensation mechanism.<sup>8,9</sup> Despite the improvement in off-state buffer leakage, the best report on the critical electric field for a single C-doped buffer layer (not an HEMT structure) is limited to 2 MV/cm.<sup>8</sup> It is worth further highlighting that a C-doped buffer layer needs to be far from the 2DEG channel of an HEMT in order to prevent the high concentration of acceptors induced by C-doping from diffusing into the 2DEG channel (otherwise, this leads to a significant reduction in sheet carrier density).<sup>9,10</sup> As a result, an undoped GaN layer prepared at a high temperature (which can significantly reduce or eliminate C-doping) is generally required prior to the growth of the AlGaIn barrier of an HEMT structure.<sup>9</sup> Of course, an increase in the undoped GaN layer thickness is more effective for stopping carbon diffusion while also enhancing the risk of a buffer leakage. Therefore, a compromise between buffer leakage and the thickness of the undoped GaN layer has to be made.<sup>9,10</sup> Consequently, the critical electric field of a full HEMT structure using the C-doped buffer approach is limited to 1.5 MV/cm, which is far below the theoretical limit of GaN.<sup>11,12</sup>

Only a few reports, which have reported a higher breakdown field of GaN than 1.5 MV/cm, are limited to a p–n junction (in a vertical architecture) grown on extremely expensive bulk GaN substrates,<sup>12–17</sup> which do not reflect the intrinsic properties of GaN due to the utilization of a p–n junction. In addition, the breakdown field is calculated depending on the accuracy of the p-doping level used in a p–n junction, and furthermore, the major advantage of the 2DEG formed as a result of the inherent polarization cannot be exploited for such a vertical architecture.

Therefore, it is crucial to explore a new growth approach to fully exploit the upper limits of intrinsic GaN for widely used lateral devices where the 2DEG formed as a result of the inherent polarization can be fully exploited.

In this study, we have explored an approach toward the limit of GaN materials by means of using our high-temperature AlN buffer, which was originally designed for the growth of novel III-nitride optoelectronics<sup>18–22</sup> instead of the classic two-step growth method, where a 2D growth mode is employed throughout the whole growth processes. A record breakdown field of 2.5 MV/cm has been demonstrated. Furthermore, high-voltage AlGaIn/GaN HEMTs with an extremely low off-state buffer leakage current of down to 1 nA/mm at up to 1000 V have been obtained.

## EXPERIMENTAL SECTION

**MOCVD Growth on *c*-Plane Sapphire Substrates.** Sample A was prepared using the classic two-step approach. The detailed growth conditions for sample A are provided in the [Supporting Information](#). Samples B to E were grown by using our high-temperature AlN buffer approach; namely, ammonia (NH<sub>3</sub>) preflow was then conducted on sapphire for nitration after the substrate was initially subjected to a high-temperature annealing process under ambient H<sub>2</sub>. A 500 nm AlN buffer layer was subsequently grown at 1180 °C followed by the growth of a 1.5 μm GaN buffer layer, then a 1 nm AlN spacer, and finally a 25 nm AlGaIn barrier (20% Al composition) all grown at 1110 °C. The detailed growth conditions for samples B–E are provided in the [Supporting Information](#). Hall measurements were

conducted on all the samples, showing a similar sheet carrier concentration of around  $9 \times 10^{12} \text{ cm}^{-2}$  with an electron mobility around  $1300 \text{ cm}^2 \text{ V}^{-1} \text{ s}^{-1}$ , while single GaN cannot achieve such a high carrier concentration and such a high mobility.

**Fabrication of AlGaIn/GaN HEMTs.** A mesa isolation was first performed using Cl<sub>2</sub>-based inductively coupled plasma (ICP) dry etching with an etch depth of 350 nm. A Ti/Al/Ni/Au alloy (20/120/20/45 nm) was then deposited using a standard thermal evaporator followed by a rapid thermal annealing process at 775 °C for 1 min in order to form ohmic contacts for source and drain electrodes. A contact resistance of 1 Ω-mm was obtained by using a transmission line measurement. A Ni/Au alloy (20 nm/200 nm) was then deposited to form Schottky contact serving as a gate electrode. Finally, bond pad metal was deposited using Ni/Au (20/200 nm) for electrical characterization.

**Breakdown Measurements.** Two isolated ohmic pads with a gap spacing of 3 μm were used to test a breakdown. A 1000 V Keithley 2410 source measure unit (SMU) was used to supply a bias between the two ohmic pads and then monitor leakage current. The bias increased from 0 V with a 5 V step size until a catastrophic breakdown occurred in device under test (DUT). The breakdown voltage was recorded and was converted to an electric field over the 3 μm gap spacing. Four terminal breakdown measurements were performed to characterize an off-state leakage current for our HEMTs. A 1000 V Keithley 2410 SMU was connected to the drain electrode of the DUT to sweep the bias from 0 to 1000 V with a 5 V step size. The gate was pinched off at  $V_{\text{GS}} = -5 \text{ V}$  using a 40 V Keithley 2602b SMU. Two Keithley 2410 and Keithley 2602b SMUs were used as ampere meters and were connected to the source and the substrate electrodes. The currents flowing through the drain, the source, the gate, and the substrate electrodes were monitored individually via the corresponding SMUs.

## RESULTS AND DISCUSSION

In order to maintain a 2D growth method and also to minimize auto carbon-doping in GaN (generally occurs at a low temperature<sup>7</sup>), high temperatures for both the growth of the thick AlN buffer (at 1180 °C) and the subsequent growth of a GaN buffer layer, then an AlN spacer, and finally an AlGaIn barrier (all at 1110 °C) are utilized. Furthermore, a low V/III ratio needs to be carefully optimized in order to facilitate a 2D growth mode throughout the whole growth processes. AlGaIn/GaN HEMTs with a depletion mode (D-mode) have been fabricated in order to characterize the electrical performance of the GaN buffer.

Figure 1 shows the schematics of a standard HEMT structure, typically consisting of a 25 nm Al<sub>0.2</sub>Ga<sub>0.8</sub>N barrier

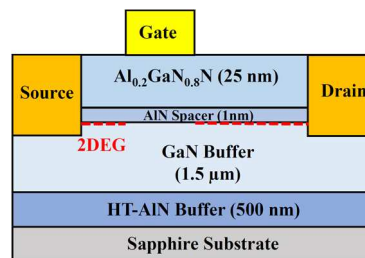
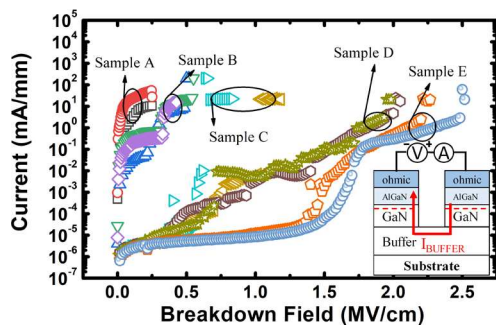


Figure 1. Schematics of our AlGaIn/GaN HEMT structure.

and a 1 nm AlN spacer in addition to the GaN buffer layer and the AlN buffer layer. The HEMT device was fabricated with a gate width of 100 μm, a gate length of 1.5 μm, a gate-drain separation ( $L_{\text{GD}}$ ) of 9 μm, and a source-drain separation of 13 μm. The larger  $L_{\text{GD}}$  implemented than the source-drain separation is to withstand high drain voltages. In order to

test the intrinsic properties of our GaN buffer, we did not use any passivation or any field plates for the fabrication of the HEMTs.

In order to examine the maximal critical electric field of our samples, two isolated ohmic contacts with a 3  $\mu\text{m}$  gap spacing have been fabricated where standard Ti/Al alloys are used for the ohmic contacts. The inset of Figure 2 schematically



**Figure 2.** Data for the breakdown field measurements for all samples where sample E shows an extremely high breakdown field of 2.5 MV/cm. Inset: schematic of our test setup for buffer leakage measurements.

illustrates our setup for our buffer leakage measurements. A bias, which is applied between the two ohmic contacts, increases until a breakdown takes place, where breakdown is defined as when the leakage current exceeds 20 mA/mm. Figure 2 shows the breakdown field results of all the samples. Two separate groups (samples A to C and samples D and E) have been identified. For sample A and samples B and C, the breakdown takes place at a bias of <300 V, meaning low breakdown fields of 0.25, 0.5, and 1 MV/cm, respectively.

In remarkable contrast, samples D and E demonstrate a high breakdown field over 2 MV/cm, in particular sample E, which

exhibits an extremely low buffer leakage of <1  $\mu\text{A}/\text{mm}$  at up to 1.65 MV/cm and a breakdown voltage of 750 V that is equivalent to an extremely high breakdown field of 2.5 MV/cm. This value approaches the theoretical limit of GaN, which is more than 1.5 times the upper limit of any existing GaN buffers including C-doped GaN buffers.

Figure 3a shows the gate transfer characteristics of our AlGaIn/GaN HEMTs fabricated on sample E as shown in the inset of Figure 3a. An output current of 370 mA/mm has been obtained at  $V_{\text{GS}} = 1$  V with a threshold voltage of around  $-3.5$  V. Figure 3b shows a typical  $I$ - $V$  characteristic, exhibiting an on-state resistance ( $R_{\text{on}}$ ) of 13  $\Omega$  mm, which is equivalent to 1.95  $\text{m}\Omega\cdot\text{cm}^2$ , considering the active region of a 1  $\mu\text{m}$  transfer length from both source and drain electrodes. Four terminal breakdown measurements as illustrated in the inset of Figure 3c have been conducted to measure the buffer leakage of the devices. The gate is pinched off at  $V_{\text{GS}} = -5$  V, while the drain is swept from 0 to 1000 V, the upper limit of the bias of our setup. The currents through the drain ( $I_{\text{total}}$ ), source ( $I_{\text{buffer}}$ ), gate ( $I_{\text{gate}}$ ), and substrate ( $I_{\text{sub}}$ ) electrodes have all been monitored, while only  $I_{\text{total}}$  and  $I_{\text{buffer}}$  have been shown for simplicity.

Figure 3c demonstrates that an extremely low off-state buffer leakage of <1 nA/mm at up to 1000 V has been achieved. The total leakage current is dominated by  $I_{\text{gate}}$  as a result of our highly resistive GaN buffer layer. Despite slight variation in  $I_{\text{total}}$ , an excellent off-state leakage current of 100 nA/mm has been achieved at 1000 V for the device with a  $L_{\text{GD}}$  of 9  $\mu\text{m}$  without any field plates. Figure 3d shows that our device demonstrates an excellent figure-of-merit ( $V_{\text{br}}^2/R_{\text{on,sp}}$ ) of  $5.13 \times 10^8$   $\text{V}^2/\Omega\cdot\text{cm}^2$  compared to existing AlGaIn/GaN HEMTs.<sup>24–35</sup>

Further material characterization has been conducted on samples D and E in order to explore the fundamental physics behind the extremely high breakdown voltage and the

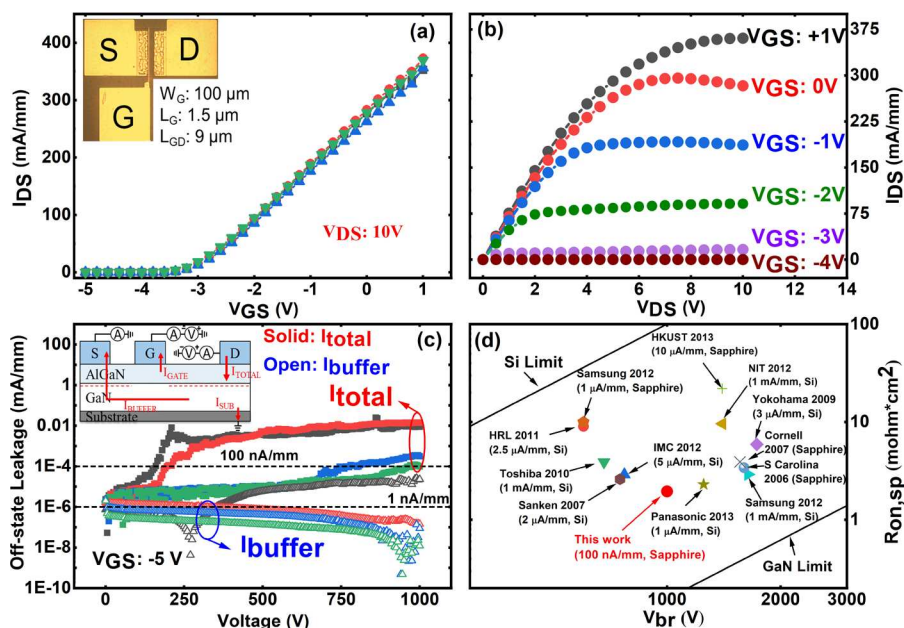


**Figure 3.** (a) Gate transfer characteristics (DC) of the devices fabricated on sample E; inset: optical image of the fabricated AlGaIn/GaN HEMT; (b)  $I$ - $V$  characteristics (DC) of the fabricated device; (c) four terminal breakdown results measured at  $V_{\text{GS}} = -5$  V and  $V_{\text{DS}}$  of up to 1000 V with monitoring current through drain ( $I_{\text{total}}$ ), source ( $I_{\text{source}}$ ), gate ( $I_{\text{gate}}$ ), and substrate ( $I_{\text{sub}}$ ) (only  $I_{\text{total}}$  and  $I_{\text{buffer}}$  are shown); inset: schematic of our terminal breakdown measurement setup; (d) benchmarking our devices against the state of the art by comparing their figures-of-merit ( $V_{\text{br}}^2/R_{\text{on,sp}}$ ).

extremely low leakage current. Figure 4a,b shows the atomic force microscopy (AFM) images of a standard GaN layer

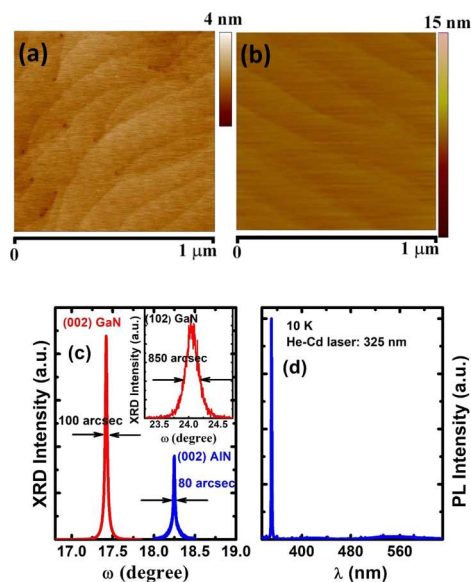


**Figure 4.** Typical AFM images of the GaN layer grown (a) using the classic two-step growth method and (b) on our HT AlN buffer; (c) XRD rocking curves of the GaN grown on our HT AlN buffer and the HT AlN buffer itself both along the (002) direction; inset: XRD rocking curve of the GaN grown on our HT AlN buffer; (d) PL spectra of the GaN grown on our HT AlN buffer, measured at 18 K using a 325 nm He-Cd laser as an excitation source.

grown using the classic two-step growth method and the GaN layer grown on our high-temperature (HT) AlN buffer in a scanning area of  $1 \times 1 \mu\text{m}^2$ , respectively. The AFM images with a larger scanning area are provided in the Supporting Information. Figure 4a shows that the standard GaN grown by using the classic two-step method typically exhibits a number of dark spots due to the termination of screw dislocations, which can be widely observed as a replica of GaN coalescence on GaN nanoislands formed from the thin LT nucleation layer due to the annealing processes mentioned above.<sup>23</sup> In remarkable contrast, Figure 4b shows the typical AFM image of the GaN grown on our HT AlN that exhibits features with parallel and straight terraces without any dark spots, demonstrating a step-flow growth mode, that is, a typical 2D layer-by-layer growth mode, which is different from the classic two-step growth.<sup>19–23</sup> These results are consistent with the X-ray diffraction (XRD) measurements performed along the (002) direction as shown in Figure 4c. The GaN on our HT AlN buffer exhibits a narrow full width at half-maximum (FWHM) of the XRD rocking curve,  $\sim 100$  arcsec, and the FWHM of the (0002) XRD rocking curve of our HT AlN buffer itself is only 80 arcsec as we reported previously.<sup>19–22</sup> The much narrower FWHM indicates a very low screw dislocation density, which has also been confirmed by our transmission electron microscopy measurements.<sup>19</sup> Note that the typical FWHM of the (0002) XRD rocking curve of standard GaN grown by the two-step method is around 250–300 arcsec.<sup>23</sup> In order to maintain a 2D growth mode, it is necessary to grow an AlN buffer layer at a very high temperature and a very low V/III ratio under a low pressure.<sup>19–22</sup> The subsequent GaN buffer growth also needs to follow a similar trend with a high growth rate. An increased

V/III ratio and a reduced growth temperature will lead to a deviation from a 2D growth mode, such as samples B and C.

Generally speaking, it has been predicted that the electrical properties of GaN are strongly affected by threading dislocations, namely, screw and edge dislocations.<sup>36,37</sup> For example, screw dislocations generally generate current leakage paths. Therefore, it is crucial to significantly reduce the density of screw dislocations in order to minimize leakage current in GaN.<sup>36,37</sup> Edge dislocations are likely to accommodate any unintentional acceptor impurities. As a result, edge dislocations with a reasonably high density can effectively suppress leakage current.<sup>37</sup> The GaN grown on our HT AlN in a 2D growth mode aligns with the two requirements. Although the FWHM of the XRD rocking curves of either the GaN or the AlN along the (002) direction is very narrow, meaning a very low screw dislocation density, the FWHM of the XRD rocking curve along the (102) direction is 850 arcsec for samples D and E as shown in the inset of Figure 4c, which is much broader than that of the standard GaN grown using the classic two-step growth method (typically  $\sim 300$  arcsec). This means that our GaN exhibits a fairly high density of edge dislocations. Therefore, our results agree with the theoretical studies,<sup>6,10,36,37</sup> confirming the influence of threading dislocations on the electrical properties of GaN. The detailed XRD rocking curves (including FWHM) of the standard GaN measured along both the (002) and the (102) directions are provided in the Supporting Information.

Further material characterization includes low-temperature photoluminescence (PL) measurements performed at 18 K. C-doped GaN typically exhibits a much stronger yellow band emission centered at 550 nm due to carbon doping induced deep levels.<sup>6,10</sup> In contrast, Figure 4d shows the PL spectrum of sample E, which exhibits a strong GaN band edge emission at 357 nm with a negligible yellow band emission at 550 nm. This means that negligible auto carbon doping was generated during the epitaxial growth processes of our GaN at a high temperature. The conclusion agrees with the fact that a high growth temperature ( $>1100$  °C) leads to a remarkable limit in carbon incorporation into GaN as a result of the increased availability of absorbed hydrogen.<sup>7</sup> The PL spectrum of the standard GaN measured at 18 K is provided in the Supporting Information.

## CONCLUSIONS

In conclusion, we have reported a record breakdown field of 2.5 MV/cm on our HEMTs grown using the undoped GaN buffer layer on our HT AlN buffer technology on sapphire, which approaches the theoretical limit of GaN and is  $>1.5$  times that of any existing GaN buffers including C-doped buffers. Our fabricated AlGaIn/GaN HEMTs with a  $L_{\text{GD}}$  of 9  $\mu\text{m}$  have demonstrated a negligible buffer leakage of 1 nA/mm at 1000 V and an excellent figure-of-merit ( $V_{\text{br}}^2/R_{\text{on,sp}}$ ) of  $5.13 \times 10^8 \text{ V}^2/\Omega\cdot\text{cm}^2$ . We believe that a 2D growth method, which benefits from our HT AlN buffer technology, makes a major contribution to the extremely high breakdown field and the extremely low leakage current. The presented results also imply that it is possible to achieve the intrinsic limits of GaN electronics by further exploring epitaxial growth on large lattice-mismatched and industry compatible substrates.

## ■ ASSOCIATED CONTENT

### Supporting Information

The Supporting Information is available free of charge at <https://pubs.acs.org/doi/10.1021/acsami.9b19697>.

Experimental section, a table of growth parameters, AFM images, and XRD curves (PDF)

## ■ AUTHOR INFORMATION

### Corresponding Author

Tao Wang – Department of Electronic and Electrical Engineering, University of Sheffield, Sheffield S1 3JD, United Kingdom; [orcid.org/0000-0001-5976-4994](https://orcid.org/0000-0001-5976-4994); Email: [t.wang@sheffield.ac.uk](mailto:t.wang@sheffield.ac.uk)

### Authors

Sheng Jiang – Department of Electronic and Electrical Engineering, University of Sheffield, Sheffield S1 3JD, United Kingdom

Yuefei Cai – Department of Electronic and Electrical Engineering, University of Sheffield, Sheffield S1 3JD, United Kingdom

Peng Feng – Department of Electronic and Electrical Engineering, University of Sheffield, Sheffield S1 3JD, United Kingdom

Shuoheng Shen – Department of Electronic and Electrical Engineering, University of Sheffield, Sheffield S1 3JD, United Kingdom

Xuanming Zhao – Department of Electronic and Electrical Engineering, University of Sheffield, Sheffield S1 3JD, United Kingdom

Peter Fletcher – Department of Electronic and Electrical Engineering, University of Sheffield, Sheffield S1 3JD, United Kingdom

Volkan Esendag – Department of Electronic and Electrical Engineering, University of Sheffield, Sheffield S1 3JD, United Kingdom

Kean-Boon Lee – Department of Electronic and Electrical Engineering, University of Sheffield, Sheffield S1 3JD, United Kingdom

Complete contact information is available at: <https://pubs.acs.org/doi/10.1021/acsami.9b19697>

### Author Contributions

†S.J. and Y.C. contributed equally to this work.

### Author Contributions

T.W. conceived the idea and organized the project. T.W., S.J., and Y.C. prepared the manuscript. S.J. fabricated devices and performed device characterization. Y.C. contributed to initial device fabrication and device testing. K.-B.L. contributed to device testing. P.Feng grew the samples. Y.C., S.S., X.Z., P.Fletcher, and V.D. performed material characterization.

### Funding

This work is supported by Engineering and Physical Sciences Research Council (EPSRC), U.K., under Grant EP/P006973/1.

### Notes

The authors declare no competing financial interest.

## ■ ACKNOWLEDGMENTS

Financial support is acknowledged from the Engineering and Physical Sciences Research Council (EPSRC), U.K., via EP/P006973/1.

## ■ REFERENCES

- (1) Ambacher, O.; Smart, J.; Shealy, J. R.; Weimann, N. G.; Chu, K.; Murphy, M.; Schaff, W. J.; Eastman, L. F.; Dimitrov, R.; Wittmer, L.; Stutzmann, M.; Rieger, W.; Hilsenbeck, J. Two-dimensional Electron Gases Induced by Spontaneous and Piezoelectric Polarization Charges in N- and Ga-face AlGa<sub>N</sub>/Ga<sub>N</sub> Heterostructures. *J. Appl. Phys.* **1999**, *85*, 3222–3233.
- (2) Jones, K. A.; Chow, T. P.; Wraback, M.; Shatalov, M.; Sitar, Z.; Shahedipour, F.; Uduary, K.; Tompa, G. S. AlGa<sub>N</sub> Devices and Growth of Device Structures. *J. Mater. Sci.* **2015**, *50*, 3267–3307.
- (3) Huang, A. Q. New Unipolar Switching Power Device Figures of Merit. *IEEE Electron Device Lett.* **2004**, *25*, 298–301.
- (4) Lee, H. P.; Perozek, J.; Rosario, L. D.; Bayram, C. Investigation of AlGa<sub>N</sub>/Ga<sub>N</sub> High Electron Mobility Transistor Structures on 200-mm Silicon (111) Substrates Employing Different Buffer Layer Configurations. *Sci. Rep.* **2016**, *6*, 37588.
- (5) Rowena, I. B.; Selvaraj, S. L.; Egawa, T. Buffer Thickness Contribution to Suppress Vertical Leakage Current with High Breakdown Field (2.3 MV/cm) for Ga<sub>N</sub> on Si. *IEEE Electron Device Lett.* **2011**, *32*, 1534–1536.
- (6) Tang, H.; Webb, J. B.; Bardwell, J. A.; Raymond, S.; Salzman, J.; Uzan-Saguy, C. Properties of Carbon-doped Ga<sub>N</sub>. *Appl. Phys. Lett.* **2001**, *78*, 757–759.
- (7) Chen, J. T.; Forsberg, U.; Janzén, E. Impact of Residual Carbon on Two-dimensional Electron Gas Properties in Al<sub>x</sub>Ga<sub>1-x</sub>N/Ga<sub>N</sub> Heterostructure. *Appl. Phys. Lett.* **2013**, *102*, 193506.
- (8) Ikeda, N.; Niiyama, Y.; Kambayashi, H.; Sato, Y.; Nomura, T.; Kato, S.; Yoshida, S. Ga<sub>N</sub> Power Transistors on Si Substrates for Switching Applications. *Proc. IEEE* **2010**, *98*, 1151–1161.
- (9) Bahat-Treidel, E.; Brunner, F.; Hilt, O.; Cho, E.; Wurfl, J.; Trankle, G. AlGa<sub>N</sub>/Ga<sub>N</sub>/Ga<sub>N</sub>:C Back-barrier HFETs with Breakdown Voltage of Over 1 kV and Low R<sub>ON</sub> × A. *IEEE Trans. Electron Devices* **2010**, *57*, 3050–3058.
- (10) Selvaraj, J.; Selvaraj, S. L.; Egawa, T. Effect of Ga<sub>N</sub> Buffer Layer Growth Pressure on the Device Characteristics of AlGa<sub>N</sub>/Ga<sub>N</sub> High-electron-mobility Transistors on Si. *Jpn. J. Appl. Phys.* **2009**, *48*, 121002.
- (11) Yang, L.; Zhang, M.; Hou, B.; Mi, M.; Wu, M.; Zhu, Q.; Zhu, J.; Lu, Y.; Chen, L.; Zhou, X.; Lv, L.; Ma, X.; Hao, Y. High Channel Conductivity, Breakdown Field Strength, and Low Current Collapse in AlGa<sub>N</sub>/Ga<sub>N</sub>/Si Delta-Doped AlGa<sub>N</sub>/Ga<sub>N</sub>:C HEMTs. *IEEE Trans. Electron Devices* **2019**, *66*, 1202–1207.
- (12) Mandal, S.; Kanathila, M. B.; Pynn, C. D.; Li, W.; Gao, J.; Margalith, T.; Laurent, M. A.; Chowdhury, S. Observation and Discussion of Avalanche Electroluminescence in Ga<sub>N</sub> p-n Diodes Offering a Breakdown Electric Field of 3 MV cm<sup>-1</sup>. *Semicond. Sci. Technol.* **2018**, *33*, No. 065013.
- (13) Wang, J.; Cao, L.; Xie, J.; Beam, E.; McCarthy, R.; Youtsey, C.; Fay, P. High Voltage, High Current Ga<sub>N</sub>-on-Ga<sub>N</sub> p-n Diodes with Partially Compensated Edge Termination. *Appl. Phys. Lett.* **2018**, *113*, No. 023502.
- (14) Nomoto, K.; Song, B.; Hu, Z.; Zhu, M.; Qi, M.; Kaneda, N.; Mishima, T.; Nakamura, T.; Jena, D.; Xing, H. G. 1.7-kV and 0.55-mΩcm<sup>2</sup> Ga<sub>N</sub> p-n Diodes on Bulk Ga<sub>N</sub> Substrates with Avalanche Capability. *IEEE Electron Device Lett.* **2016**, *37*, 161–164.
- (15) Kizilyalli, I. C.; Edwards, A. P.; Aktas, O.; Prunty, T.; Bour, D. Vertical Power p-n Diodes Based on Bulk Ga<sub>N</sub>. *IEEE Trans. Electron Devices* **2014**, *62*, 414–422.
- (16) Hilt, O.; Treidel, E. B.; Wolf, M.; Kuring, C.; Tetzner, K.; Yazdani, H.; Wentzel, A.; Würfl, J. Lateral and Vertical Power Transistors in Ga<sub>N</sub> and Ga<sub>2</sub>O<sub>3</sub>. *IET Power Electron.* **2019**, *12*, 3919–3927.

- (17) Lee, M.; Mikulik, D.; Yang, M.; Park, S. The Investigation of Stress in Freestanding GaN Crystals Grown from Si Substrates by HVPE. *Sci. Rep.* **2017**, *7*, 8587.
- (18) Wang, T.; Bai, J.; Parbrook, P. J.; Cullis, A. G. Air-bridged Lateral Growth of an Al<sub>0.98</sub>Ga<sub>0.02</sub>N Layer by Introduction of Porosity in an AlN Buffer. *Appl. Phys. Lett.* **2005**, *87*, 151906.
- (19) Bai, J.; Wang, T.; Parbrook, P. J.; Lee, K. B.; Cullis, A. G. A Study of Dislocations in AlN and GaN Films Grown on Sapphire Substrates. *J. Cryst. Growth* **2005**, *282*, 290–296.
- (20) Wang, Q.; Wang, T.; Bai, J.; Cullis, A. G.; Parbrook, P. J.; Ranalli, F. Growth and Optical Investigation of Self-assembled InGaN Quantum Dots on a GaN Surface Using a High Temperature AlN Buffer. *J. Appl. Phys.* **2008**, *103*, 123522.
- (21) Wang, Q.; Gong, Y. P.; Zhang, J. F.; Bai, J.; Ranalli, F.; Wang, T. Stimulated Emission at 340 nm from AlGaIn Multiple Quantum Wells Grown Using High Temperature AlN Buffer Technologies on Sapphire. *Appl. Phys. Lett.* **2009**, *95*, 161904.
- (22) Davies, S. C.; Mowbray, D. J.; Wang, Q.; Ranalli, F.; Wang, T. Influence of Crystal Quality of Underlying GaN Buffer on the Formation and Optical properties of InGaIn/GaN Quantum Dots. *Appl. Phys. Lett.* **2009**, *95*, 101909.
- (23) Wang, T.; Shirahama, T.; Sun, H. B.; Wang, H. X.; Bai, J.; Sakai, S.; Misawa, H. Influence of Buffer Layer and Growth Temperature on the Properties of an Undoped GaN Layer Grown on Sapphire Substrate by Metalorganic Chemical Vapor Deposition. *Appl. Phys. Lett.* **2000**, *76*, 2220–2222.
- (24) Van Hove, M.; Boulay, S.; Bahl, S. R.; Stoffels, S.; Kang, X.; Wellekens, D.; Geens, K.; Delabie, A.; Decoutere, S. CMOS Process-compatible High-power Low-leakage AlGaIn/GaN MISHEMT on Silicon. *IEEE Electron Device Lett.* **2012**, *33*, 667–669.
- (25) Iwakami, S.; Machida, O.; Yanagihara, M.; Ehara, T.; Kaneko, N.; Goto, H.; Iwabuchi, A. 20 mΩ, 750 V High-power AlGaIn/GaN Heterostructure Field-effect Transistors on Si Substrate. *Jpn. J. Appl. Phys.* **2007**, *46*, L587.
- (26) Saito, W.; Kakiuchi, Y.; Nitta, T.; Saito, Y.; Noda, T.; Fujimoto, H.; Yoshioka, A.; Ohno, T.; Yamaguchi, M. Field-plate Structure Dependence of Current Collapse Phenomena in High-voltage GaN-HEMTs. *IEEE Electron Device Lett.* **2010**, *31*, 659–661.
- (27) Chu, R.; Corrión, A.; Chen, M.; Li, R.; Wong, D.; Zehnder, D.; Hughes, B.; Boutros, K. 1200-V Normally-off GaN-on-Si Field-effect Transistors with Low Dynamic on-resistance. *IEEE Electron Device Lett.* **2011**, *32*, 632–634.
- (28) Lee, J. H.; Jeong, J. H.; Lee, J. H. Normally-off GaN Power MOSFET Grown on Sapphire Substrate with Highly Resistive Undoped Buffer Layer. *IEEE Electron Device Lett.* **2012**, *33*, 1429–1431.
- (29) Liu, X.; Zhan, C.; Chan, K. W.; Owen, M. H. S.; Liu, W.; Chi, D. Z.; Tan, L. S.; Chen, K. J.; Yeo, Y. C. AlGaIn/GaN Metal-oxide-semiconductor High-electron-mobility Transistors with a High Breakdown Voltage of 1400 V and a Complementary Metal-oxide-semiconductor Compatible Gold-free process. *Jpn. J. Appl. Phys.* **2013**, *52*, No. 04CF06.
- (30) Selvaraj, S. L.; Watanabe, A.; Wakejima, A.; Egawa, T. 1.4-kV Breakdown Voltage for AlGaIn/GaN High-electron-mobility Transistors on Silicon Substrate. *IEEE Electron Device Lett.* **2012**, *33*, 1375–1377.
- (31) Ikeda, N.; Kaya, S.; Li, J.; Kokawa, T.; Masuda, M.; Katoh, S. High-power AlGaIn/GaN MIS-HFETs with Field-plates on Si Substrates. *Int. Symp. Power Semicond. Devices IC's* **2009**, 251–254.
- (32) Choi, Y. C.; Shi, J.; Pophristic, M.; Spencer, M. G.; Eastman, L. F. C-doped Semi-insulating GaN HFETs on Sapphire Substrates with a High Breakdown Voltage and Low Specific on-resistance. *J. Vac. Sci. Technol.* **2007**, *25*, 1836–1841.
- (33) Tipirneni, N.; Koudymov, A.; Adivarahan, V.; Yang, J.; Simin, G.; Khan, M. A. The 1.6-kV AlGaIn/GaN HFETs. *IEEE Electron Device Lett.* **2006**, *27*, 716–718.
- (34) Hwang, I.; Choi, H.; Lee, J.; Choi, H. S.; Kim, J.; Ha, J.; Um, C. Y.; Hwang, S. K.; Oh, J.; Kim, J. Y.; Shin, J. K. 1.6 kV, 2.9 mΩcm<sup>2</sup> Normally-off p-GaN HEMT Device. *Int. Symp. Power Semicond. Devices & IC's* **2012**, 41–44.
- (35) Ishida, M.; Ueda, T.; Tanaka, T.; Ueda, D. GaN on Si Technologies for Power Switching Devices. *IEEE Trans. Electron Devices* **2013**, *60*, 3053–3059.
- (36) Usami, S.; Ando, Y.; Tanaka, A.; Nagamatsu, K.; Deki, M.; Kushimoto, M.; Nitta, S.; Honda, Y.; Amano, H.; Sugawara, Y.; Yao, Y.-Z.; Ishikawa, Y. Correlation between Dislocations and Leakage Current of p-n Diodes on a Free-standing GaN Substrate. *Appl. Phys. Lett.* **2018**, *112*, 182106.
- (37) Wong, Y. Y.; Chang, E. Y.; Yang, T. H.; Chang, J. R.; Ku, J. T.; Hudait, M. K.; Chou, W. C.; Chen, M.; Lin, K. L. The Roles of Threading Dislocations on Electrical Properties of AlGaIn/GaN Heterostructure Grown by MBE. *J. Electrochem. Soc.* **2010**, *157*, H746–H749.